

Modelling Protogalactic Collapse and Magnetic Field

Evolution with FLASH

Chris Orban

May 7, 2004

Abstract

The origin and evolution of galactic magnetic fields poses a difficult theoretical problem. In spiral galaxies, the $\alpha\omega$ dynamo effect has been successful in explaining a majority of observations, but the dynamo requires a seed field to be amplified to the magnetic field strengths observed today. Previous studies have shown that shocks in the gas that generate magnetic fields in an effect called the Biermann battery may be a significant source of the seed field. Other candidates for the source of the seed field include dwarf galaxies with strong magnetic fields accreting on to the larger galaxy. In the summer of 2004, Astronomy Professor Paul Ricker and I will utilize FLASH, a modular astrophysical code, to follow galactic magnetic field evolution beginning from the collapse of a protogalaxy, and plan to investigate the source of the seed field. The FLASH code uses a recent advance in numerical methods called adaptive mesh refinement to allow galactic magnetic fields to be investigated to a much finer degree with less computational cost than previous efforts. An introduction to magnetohydrodynamics as well as a qualitative explanation of the $\alpha\omega$ dynamo effect are also discussed in this paper.

1 Introduction

The role of magnetic fields in astrophysical environments is becoming increasingly relevant to our understanding of the universe. The first detection of astrophysical magnetic fields came in 1892 when George Ellery Hale observed intense magnetic fields in sunspots by the Zeeman effect. The birth of radio astronomy in the 1930s by Karl Jansky opened the door to the possibility of investigating astrophysical magnetic fields in more detail by detecting the galactic center's radio emission, and the Voyager missions to Jupiter, Saturn, Uranus and Neptune were instrumental in expanding our knowledge of planetary magnetic fields in the 1970s and 1980s. Advances in ground-based radio astronomy have allowed magnetic fields in our own Galaxy as well as in other galaxies to be investigated. Section 3 discusses those observations in the context of the $\alpha\omega$ dynamo.

A theoretical picture has emerged where Maxwell's equations have been joined with hydrodynamics and applies to all of the observations mentioned. This theory is appropriately called magnetohydrodynamics (MHD) and both analytic and numerical methods are used to find solutions to these equations.

2 Magnetohydrodynamics

The principal assumption of MHD is that in plasmas the electrons and ions flow together as a single fluid. Although the plasma is ionized, this assumption is justified since separating a significant number of electrons from the ions would result in an extremely strong Coulomb attraction between the two parts. This assumption also implies that on large scales the electric field is zero, and that the displacement current (proportional to the change in the electric field with time) is negligible. Also, since the plasma is treated as a single fluid, the electrons can be considered to "follow" the heavier ions so \mathbf{v} is

simply the velocity of the ions. Thus Maxwell's equations (in Gaussian units) become:

$$\nabla \cdot \mathbf{E} = 4\pi\rho \quad (1)$$

$$\nabla \times \mathbf{E} = -\frac{1}{c} \frac{\partial \mathbf{B}}{\partial t} \quad (2)$$

$$\nabla \cdot \mathbf{B} = 0 \quad (3)$$

$$\nabla \times \mathbf{B} = \frac{4\pi}{c} \mathbf{J} \quad (4)$$

$$\mathbf{J} = \sigma \left(\mathbf{E} + \frac{\mathbf{v}}{c} \times \mathbf{B} \right) \quad (5)$$

By solving for \mathbf{E} in Eq. (5) and substituting into Eq. (2), an equation coupling the \mathbf{B} field with the velocity, \mathbf{v} , is found. This coupling is responsible for “flux freezing” which strongly associates magnetic field lines to plasmas. This effect causes both to move together in an applied field such as gravity, or in situations when the twisting of the magnetic field is severe. Under the assumption that the plasma has negligible resistance (which is common in astrophysical environments), the conductivity σ is infinite and Eqs. (2) and (5) can be rearranged to become

$$\frac{\partial \mathbf{B}}{\partial t} + \nabla \times (\mathbf{B} \times \mathbf{v}) = 0. \quad (6)$$

Equation (6) bears some resemblance to the mass conservation equation, which happens to be the first equation of hydrodynamics,

$$\frac{\partial \rho}{\partial t} + \nabla \cdot (\rho \mathbf{v}) = 0, \quad (7)$$

where ρ is the density and \mathbf{v} is the velocity. Equation (6) involves the conservation of a quantity related to \mathbf{B} and \mathbf{v} . This coupling of the \mathbf{B} field with the velocity in flux freezing is an important concept, because the magnetic field of a galaxy is “frozen” into the plasma, causing the field lines to become warped and twisted as the galaxy rotates.

Maxwell's equations combined with the momentum and energy conservation equations of hydrodynamics yield the equations of MHD (in Gaussian units):

$$\frac{\partial \mathbf{B}}{\partial t} + \nabla \times (\mathbf{B} \times \mathbf{v}) = -\nabla \times (\eta \nabla \times \mathbf{B}), \quad (8)$$

$$\nabla \cdot \mathbf{B} = 0, \quad (9)$$

$$\frac{\partial \rho}{\partial t} + \nabla \cdot (\rho \mathbf{v}) = 0, \quad (10)$$

$$\frac{\partial \rho \mathbf{v}}{\partial t} + \nabla \cdot (\rho \mathbf{v} \mathbf{v}) = -\nabla P + \frac{1}{4\pi} (\nabla \times \mathbf{B}) \times \mathbf{B}, \quad (11)$$

$$\frac{\partial \rho \mathbf{E}}{\partial t} + \nabla \cdot [(\rho \mathbf{E} + P) \mathbf{v}] = \frac{\eta}{4\pi} |\nabla \times \mathbf{B}|^2. \quad (12)$$

where $\eta = c^2/(4\pi\sigma)$ is the electrical resistivity. These coupled, non-linear equations are often difficult to solve analytically so numerical methods are often employed in solving them. The $\alpha\omega$ dynamo is an analytic solution to these equations, relying on the high degree of symmetry in spiral galaxies as a simplifying factor.

3 The $\alpha\omega$ dynamo

Radio observations of galaxies have revealed a wealth of information about galactic magnetic fields. The radio waves are generated through synchrotron radiation caused by the spiraling of high-energy electrons around magnetic fields. The gyro-frequency, which is the frequency of a particle circulating around a \mathbf{B} field, for electrons is given by

$$\nu_{g,e} = \frac{eB}{2\pi m_e} \quad (13)$$

The power of the observed electromagnetic waves peaks at $\nu \sim \frac{3}{2}\gamma^2\nu_{g,e}$ where γ is just the Lorentz factor for the high-energy electrons. The strength of galactic magnetic fields (which ranges from 5-15 μG for spirals) and energies of the relativistic electrons place this frequency in the radio range.

Synchrotron radiation is highly polarized and carries the imprint of the magnetic field that the electrons were travelling in. The polarization angle of the radiation is rotated by the interaction between the electric field vector and the parallel component of the magnetic field B_{\parallel} between the source and the earth. Astronomers can correct for this effect, called Faraday rotation. The angle of rotation ϕ of the polarization vector is given by

$$\phi = R_M \lambda^2 \quad (14)$$

where

$$R_M = \frac{e^2}{2\pi m_e^2 c^4} \int n_e B_{\parallel} ds \quad (15)$$

The coefficient R_M is known as the rotation measure of the path. The integral is over a path, s , along the line of sight, and n_e is the number density of electrons. By observing at multiple wavelengths, astronomers can determine R_M and correct for the rotation of the polarization vector to find the orientation of the magnetic field at the source.

Figures 1 and 2 present radio observations of the galaxies NGC 4361 and M 51. In Fig. 1, NGC 4631 is shown with the overall radio power in color, and the field lines (determined from correcting the polarization angles) appear as vectors. The length of the vectors are proportional to the strength of the magnetic field. In contrast to Fig. 1, the same observational method applied to M 51, and using the same plotting conventions yields a much different picture as seen in Fig. 2. The orientation of these galaxies allow the overall shape of the magnetic field structure to be seen more easily. The edge-on orientation of NGC 4631 makes it easier to view the toroidal (or doughnut) shape of its magnetic field, whereas M 51 has a magnetic field which follows the spiral shape of the galaxy. The magnetic field of M 51 is representative as a poloidal field.

The $\alpha\omega$ dynamo provides an explanation to these representative cases. Figure 3 from

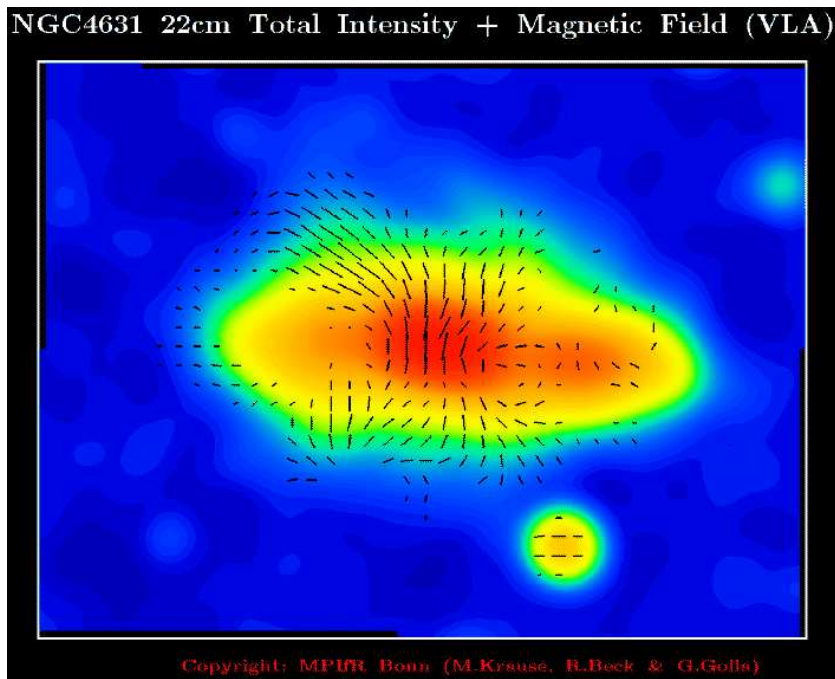


Figure 1: A radio observation of NGC 4631 taken with the Very Large Array (VLA) at a wavelength of 22 cm. Intensity is presented in color (ranging from the strongest emission indicated in red to the background level shown in blue) and magnetic field lines are indicated by vectors. (Courtesy of the Max-Planck-Institute für Radioastronomie)

Widrow (2002) shows a toroidal magnetic field at (a), perhaps not unlike the field of NGC 4631. Flux freezing drags the field lines along with the rotation of the galaxy, which spins faster in the center than the edge. This differential rotation tangles the field lines as seen in (b), which eventually settle into a poloidal symmetry at (c), much like M 51. Then supernovae explosions blast hot plasma up out of the disk of the galaxy in (d), carrying the magnetic field along with the plasma because of flux freezing. The rotation now twists the loops in the field caused by the explosion through the Coriolis effect. This twisting eventually becomes severe enough that the field reverts back into a toroidal shape in (f).

Another important feature of the $\alpha\omega$ dynamo is that the magnetic flux is amplified with time as the galaxy continues its rotation and twisting of the field lines. This also

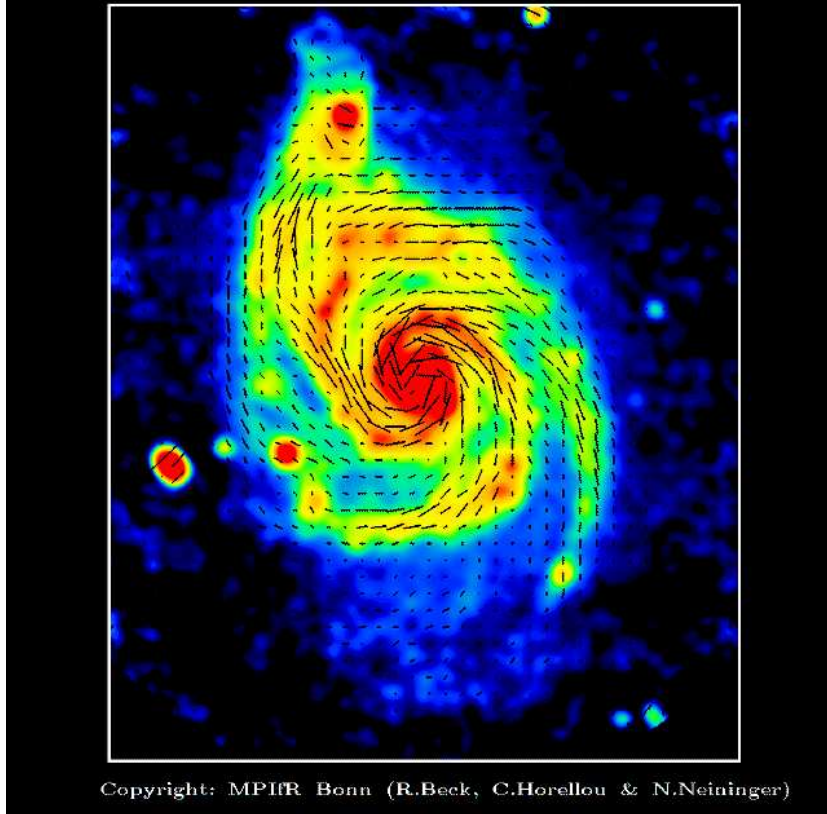


Figure 2: A radio observation of M 51 at 6 cm taken with the VLA. Intensity is indicated with color (ranging from the strongest emission indicated in red to the background level shown in black) and the magnetic field lines are indicated by vectors.(Courtesy of the Max-Planck-Institute für Radioastronomie)

imposes the condition that there must be a weak magnetic field to “seed” the $\alpha\omega$ dynamo for this amplification. In other words, if $\mathbf{B} = 0$ initially, without other physics such as the Biermann battery, the \mathbf{B} field will be zero throughout the evolution of the galaxy.

The $\alpha\omega$ dynamo has been very successful in explaining the magnetic field structure of spiral galaxies. It is an analytic solution to the MHD equations that makes use of the high degree of symmetry exhibited in spirals, and assumes that the magnitude of the \mathbf{B} field is zero outside the galactic disk. These assumptions make it difficult to apply to systems without symmetric ordered motion, such as dwarf galaxies like NGC 4449

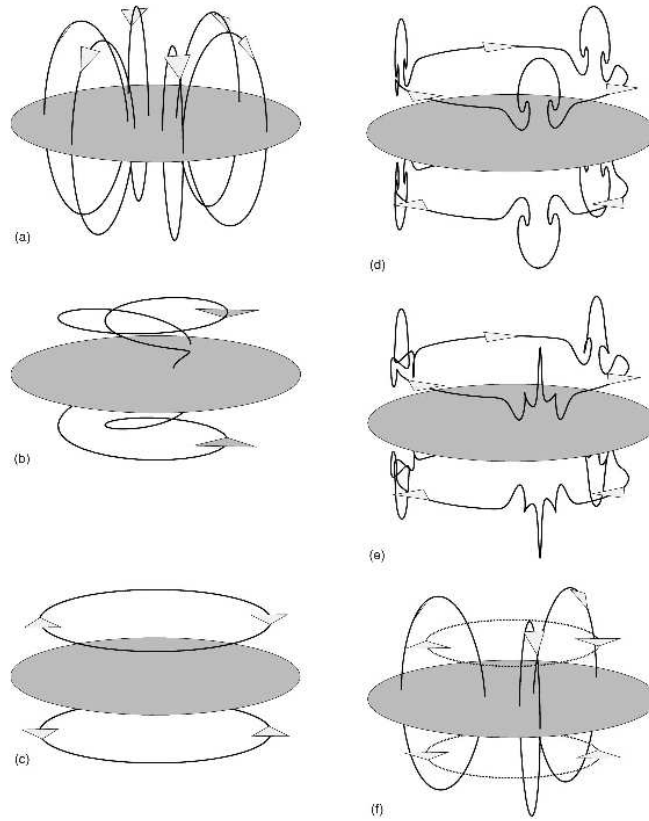


Figure 3: The sequence of magnetic field evolution in spiral galaxies according to the $\alpha\omega$ dynamo model. A toroidally shaped field in (a) through flux freezing evolves into a poloidal field in (c) and back again through supernovae explosions and the Coriolis effect, eventually reverting back to a toroidally shaped field in (f). (Courtesy of Widrow (2002))

which exhibits a magnetic field strength of $14\mu G$ (Chyzy et. al 2000).

Numerical simulations may be the only way to understand more about magnetic field evolution. Numerical modelling can also shed light on the source of the seed field. The Biermann battery effect, which will be discussed in more detail in section 5, has been studied as one a possible source of this seed field. The origin of the seed field is a significant problem in completing the picture of the galactic dynamo.

4 Numerical Methods

Solving the MHD equations for a system as complicated as a galaxy can be a difficult task. Fortunately there is no need to “reinvent the wheel”; a number of codes exist for such a task. The FLASH code is a well-tested and versatile code for astrophysics simulations. Though originally developed to simulate white dwarfs, neutron stars, and supernovae, it may also be used to investigate cosmology and galactic dynamics problems as well. Computationally, FLASH has advantages in its modular design, giving it the flexibility to turn physical effects “on” and “off” as needed, and it can be configured to include effects specified by the user which may not already be built into the code. The FLASH code is also convenient in that the code is primed for parallel processing across multiple CPUs, but the greatest computational advantage may be in adaptive mesh refinement (AMR).

Adaptive mesh refinement is a numerical technique that scales the resolution (i.e. the size of the discrete volume elements which the differential equation is approximated over) of the simulation to increase resolution in complex areas, instead of wasting computational power on less interesting parts of the simulation. Increasing the resolution gives a better approximation to the differential equations. Figure 4 is an example of this method. It is a FLASH simulation of the interaction between two fluids of different densities under a uniform gravitational acceleration. Turbulence of this type is called a Raleigh-Taylor instability. Notice that the AMR blocks become finer as the boundary between the fluids becomes more complex.

The FLASH code also holds the advantage that it is well tested, with a team devoted to testing its accuracy at the Accelerated Strategic Computing Initiative (ASCI) FLASH center at the University of Chicago, where FLASH is maintained. In fact, FLASH simulations can even be compared to laboratory experiments as another means of verifying

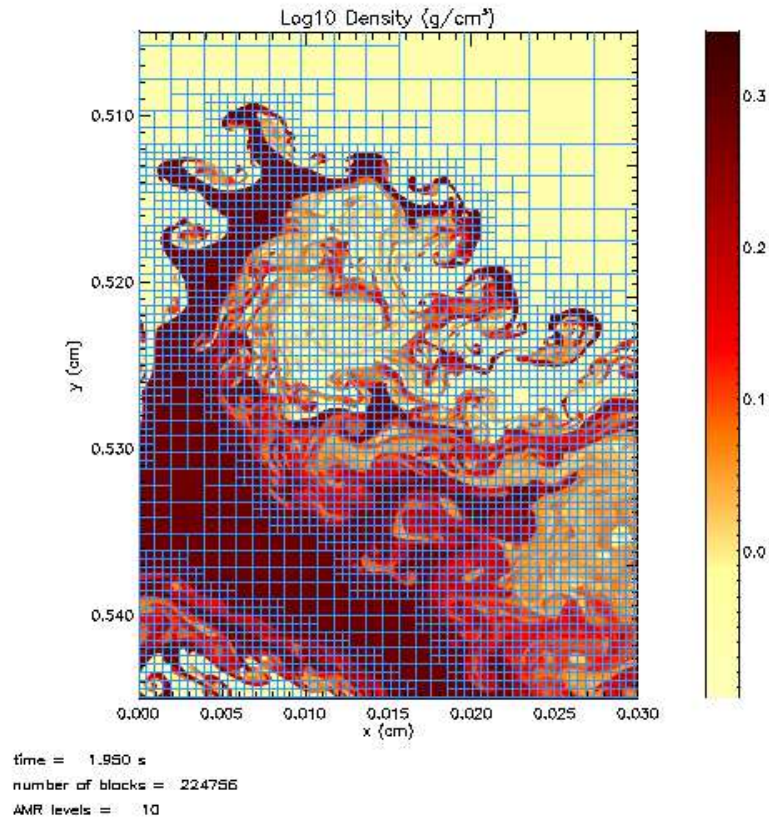


Figure 4: A simulation of two interacting fluids exhibiting Rayleigh-Taylor instability. The adaptive mesh refinement blocks are shown superimposed on the figure. (Image Copyright 1999 ASCI Flash Center)

and validating the code. Caulder et al., (2002) compares laboratory measurements of the Raleigh-Taylor instability and laser-driven shock waves to the predictions of FLASH simulations. These tests provide some perspective to more exotic situations such as the turbulent mixing of white dwarf material, or shock waves from supernovae, for example.

5 Summer Research

In the summer of 2004, Astronomy Professor Paul Ricker and I plan to model the collapse of a protogalaxy using FLASH. This protogalaxy is simply an elliptically shaped assemblage of gas and dark matter having the mass of a galaxy (i.e. within a few orders of magnitude of 10^9 solar masses). The gas is randomly perturbed to break the symmetry of

the calculation and mimic an actual astrophysical object. We are particularly interested in the seed field that is amplified by the $\alpha\omega$ dynamo. Understanding the seed field is critical to explaining the strength of observed magnetic fields in spiral galaxies which range from 5-15 μG (Chyzy et. al 2003).

This problem of protogalactic collapse has been addressed by a number of previous studies. Bertschinger (1985) investigated the very general case of the collapse of a gas cloud without including magnetic fields (but including hydrodynamics). Both analytic and numerical methods were used to study the dynamics of the collapsing gas of different collisional properties and ratios of specific heats γ . His results can be applied to a wide range of length scales, including protogalactic collapse.

Davies and Widrow (2000) built on Bertschinger's results and specifically investigated the problem of protogalactic collapse. They studied the vorticity (also called circulation) of an elliptically shaped collapsing gas cloud to learn more about the magnetic field evolution by inferring the magnetic field from the vorticity. Vorticity is defined as the curl of the velocity field, \mathbf{v} .

$$\boldsymbol{\omega} \equiv \nabla \times \mathbf{v}. \quad (16)$$

The method of using the vorticity to track the \mathbf{B} field implies that the magnetic field pressure does not affect the dynamics of the gas appreciably. This means that when reevaluating the MHD equations in terms of the vorticity, the magnetic pressure terms, such as the \mathbf{B} field term in Eq. (11), can be neglected. Under these assumptions and the assumption the gas pressure is barotropic (i.e. only dependent on pressure), combining Eqs. (10) and (11) in terms of the vorticity gives the following relation in “typical” (or non-shocked) astrophysical environments,

$$\frac{\partial \boldsymbol{\omega}}{\partial t} + \nabla \times (\boldsymbol{\omega} \times \mathbf{v}) = 0. \quad (17)$$

Equation (17) implies that vorticity is conserved the same way that the \mathbf{B} field is coupled to \mathbf{v} in flux freezing (see Eq. (6)). Equation (17) can also be thought of as conservation of circulation in a fluid. A more general treatment, which applies to “atypical” environments such as shocks as well as the “typical” environment, shows that a term proportional to $(\nabla\rho \times \nabla P)/\rho^2$ is added to the right hand side of Eq. (17) (this releases the condition that the gas is barotropic). Biermann (1950) showed that for electron-ion fluids, a more accurate derivation for Eq. (5) creates a term proportional to $(\nabla n_e \times \nabla P_e)/n_e^2$ on the right hand side of Eq. (6). Biermann’s result, referred to as the Biermann battery, is general for “typical” environments as well as shocks. Since the vorticity and magnetic field are guided by similar equations, the magnetic field can be inferred from vorticity with the relation

$$\mathbf{B} = \alpha\omega \approx 10^{-4}\omega \quad (18)$$

where \mathbf{B} is in units of gauss and ω is in units of hertz. The constant α is determined from the ratio of the extra terms that were brought in to generalize Eqs. (6) and (17) (and specifically from the proportionality between the electron number density n_e and electron pressure P_e to the actual density ρ and pressure P , assuming overall charge neutrality). Equation (18) is valid with the only approximations that the conductivity of the plasma is infinite, diffusive effects are negligible, and that initially \mathbf{B} and ω are zero.

Davies and Widrow (2000) found that vorticity increased behind shocks in the gas, which “generate” magnetic fields accordingly by Eq. (18). They conclude that the Biermann battery is a good candidate for generating seed fields early in the collapse, allowing more time for the $\alpha\omega$ dynamo to amplify the field, and that the Biermann battery alone should provide a sufficient seed field to produce microgauss magnetic fields in mature galaxies, but more work needs to be done.

In Ricker, Widrow, and Dodelson (2000), a different numerical approach, called the piecewise-parabolic method (PPM), was used to simulate the same phenomenon. The advantage in PPM over the smoothed-particle hydrodynamics code used in Davies and Widrow (2000) lies in its ability to simulate discontinuities with more accuracy. This advantage allowed the shocks to be simulated more realistically.

My work this summer will continue build on these efforts using FLASH, which offers the advantage of using AMR on this problem to achieve higher resolutions at less computational cost. In addition to confirming the results of previous studies, we will investigate the effect of dwarf galaxies with strong magnetic fields accreting into the larger galaxy as another source of the seed field. Until fairly recently, dwarf galaxies were thought to have weak magnetic fields. The discovery of NGC 4449's $14 \mu G$ field (Chyzy et. al 2000), along with other observations, has made dwarf galaxies worthy of investigation as a source of seed fields. By expanding on previous studies with advances in numerical methods, and increased computational power our goal is to continue to complete the picture of galactic magnetic fields by investigating the effects mentioned in this review and others.

6 References

- Bertschinger, E., 1985, *Astrophys. J., Suppl. Ser.* 58, 39.
- Biermann, L. 1950, *Z. Naturforsch.* 5A, 65.
- Calder, A. C. et al. 2002, *ApJS*, 143, 201.
- Chyzy, K.T., R. Beck, S. Kohle, U. Klein, and M. Urbanik, 2000, *Astron. Astrophys.* 355, 128.
- Chyzy, K.T., J. Kapik, D.J. Bomans, U. Klein. 2003, *Astron. Astrophys.* 405, 513.

Davies, G. and Widrow, L.M. 2000, *Ap. J.*, 540, 755.

Ricker, P.M., Widrow, L., and Dodelson, S. 2000, poster at Victoria Computational
Cosmology Conference, Victoria, BC.

Widrow, L.M. 2002, *Rev. Mod. Phys.*, 74, 755.